5.3 Kontrolle raumzeitlicher Oszillationen in raum-zeitlichen Systemen

1. Halbleiter-Übergitter

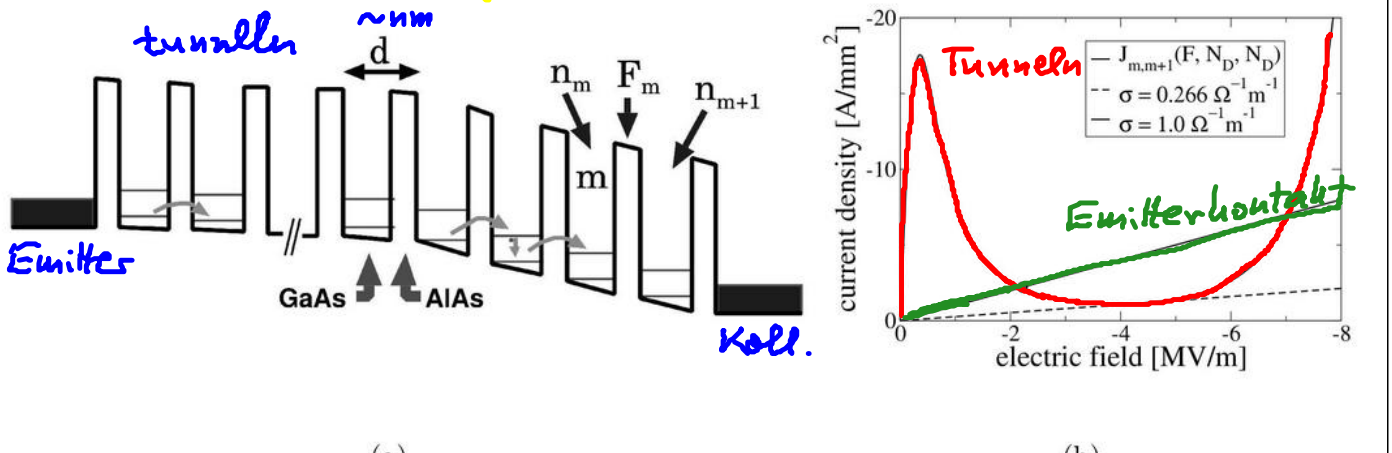

(a) (b)

FIG. 1 (a) Superlattice energy band structure of alternating GaAs and AlAs layers under bias. (b) Current density vs electric field characteristic at the emitter barrier (straight line) and between two neutral wells exhibiting negative differential conductivity.

Hizanidis, Balanov, Amann, Schöll: PRL 96, 244104 (2006)

$$\varepsilon_r \varepsilon_0 (F_m - F_{m-1}) = e(n_m - N_D) \qquad m = 1, \dots, N$$

(diskretes Gauß-Gesetz)
($e<0$, Dotierung N_D)

$$e\dot{n}_m = J_{m-1 \to m} + D\xi_m(t) - J_{m \to m+1} - D\xi_{m+1}(t)$$

(Ladungsträger-Kontinuitäts-gl. mit Gauß'schen weißen Rauschen $\langle \xi_m(t) \rangle = 0$, $\langle \xi_m(t) \xi_{m'}(t') \rangle = \delta(t-t')\delta_{mm'}$)

resonante Tunnelstromdichte J, shot noise, thermal noise

Anwendung: Hochfrequenzoszillator

D = 0 : stationäre Felddomänen → laufende Domänen

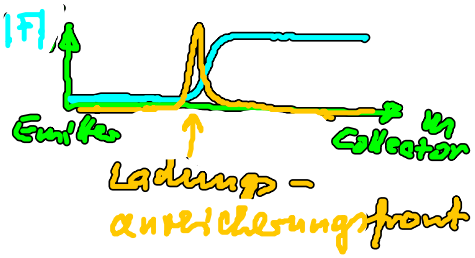

SNIPER-Bif.
(wie gener. Modell in 5.2)

globale Bedingung: Spannung $U = -\sum_{m=0}^{N} F_m d$

Ohm'sche Randbed. $J_{0\to 1} = \sigma F_0$

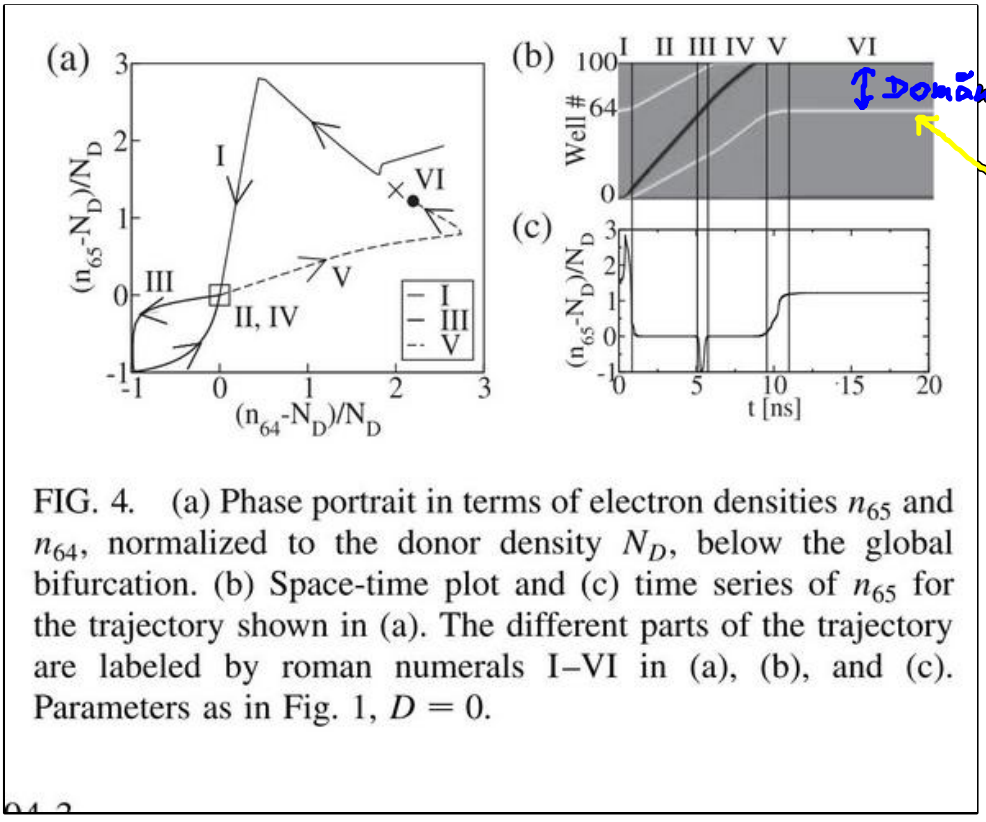

FIG. 4. (a) Phase portrait in terms of electron densities n_{65} and n_{64}, normalized to the donor density N_D, below the global bifurcation. (b) Space-time plot and (c) time series of n_{65} for the trajectory shown in (a). The different parts of the trajectory are labeled by roman numerals I–VI in (a), (b), and (c). Parameters as in Fig. 1, $D = 0$.

↕ Domäne

Anreicherungsfront

D ≠ 0 : rauschinduzierte Domänenbewegung

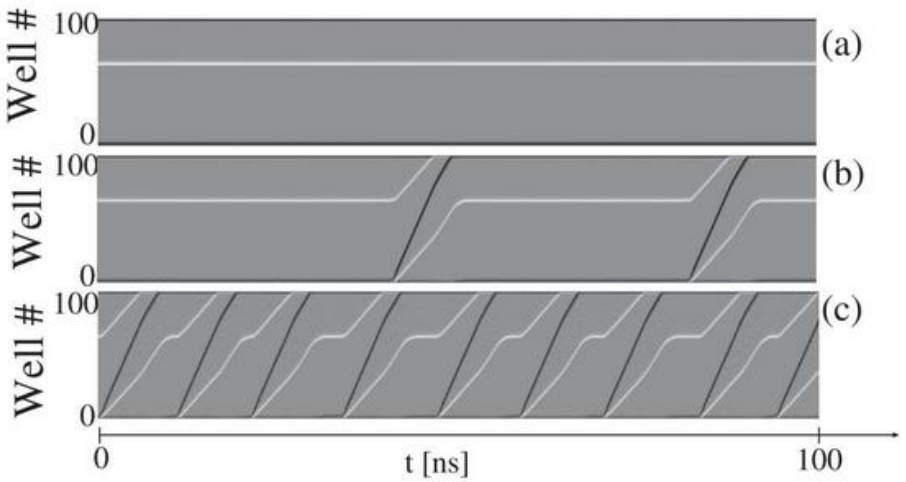

FIG. 1. Noise-induced front motion: Space-time plots of the electron density for (a) $D = 0$ (no noise), (b) $D = 0.5$ A s$^{1/2}$/m^2, and (c) $D = 2.0$ A s$^{1/2}$/m^2. Light and dark shading corresponds to electron accumulation and depletion fronts, respectively. The emitter is at the bottom. Parameters: $U = 2.99$ V, $\sigma = 2.082\,101\,248\,8\ \Omega^{-1}\,\mathrm{m}^{-1}$, $N_D = 10^{11}$ cm^{-2}, $T = 20$ K, $N = 100$ GaAs wells of width $w = 8$ nm, and $Al_{0.3}Ga_{0.7}As$ barriers of width $b = 5$ nm, energies $E^a = 41.5$ meV, $E^b = 160$ meV, scattering width $\Gamma = 8$ meV, transition matrix elements $H^{a,b}_{m,m+1} = -eF_m \times 0.0127$ m, $H^{a,a}_{m+1,m} = -0.688$ meV, $H^{b,b}_{m+1,m} = 1.263$ meV, as in Ref. [9].

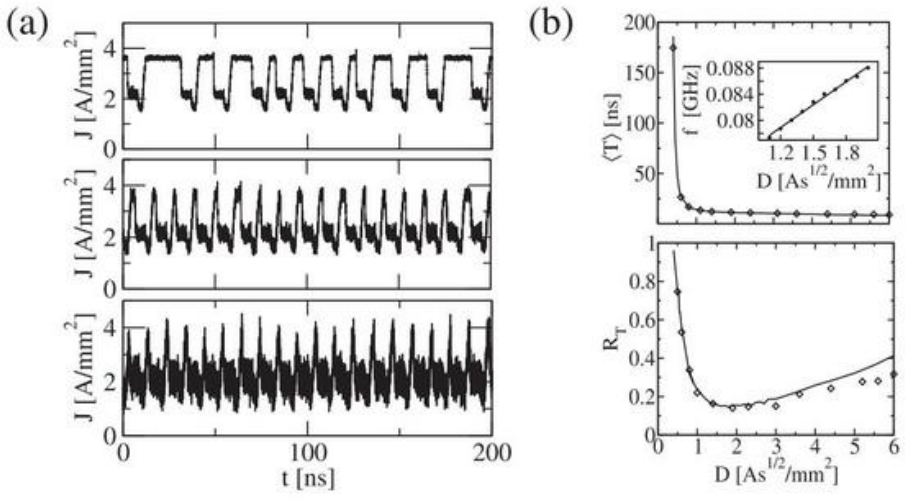

FIG. 2. (a) Three noise realizations of the current density $J(t)$. From top to bottom, $D = 0.8$, $D = 2.0$, and $D = 5.0$ A s$^{1/2}$/m^2. (b) Mean interspike interval (top panel) and its normalized fluctuations R_T (bottom panel) versus noise intensity. Lines, constant D; diamonds, $D \sim J^{1/2}_{m-1\to m}$ [18]. The inset shows the peak frequency versus D.

Rückkopplungskontrolle

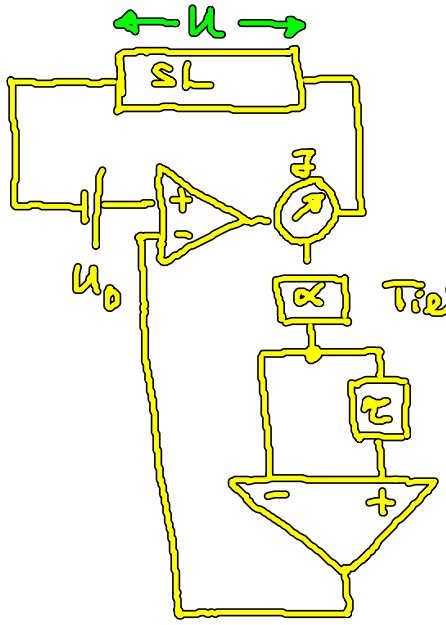

$$u = u_0 - K\,[\bar{J}(t) - \bar{J}(t-\tau)]$$

Tiefpassfilter $\bar{J} = \alpha \int_0^t J(t)\, e^{-\alpha(t-t')}\, dt'$

(Abschneidefrequenz α)

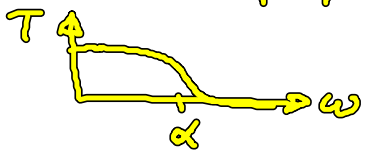

$$J = \frac{1}{N+1} \sum_{n=0}^{N} J_{n \to n+1}$$

Gesamtstrom (ind. Verschiebungsstrom)

- delay-induz. Koexistenz Bif. zu kurz. Domänen (wie im gener. SNIPER-Modell)
- Kontrolle der Kohärenzresonanz

Hizanidis & Schöll, PRE 78, 066205 (2008)

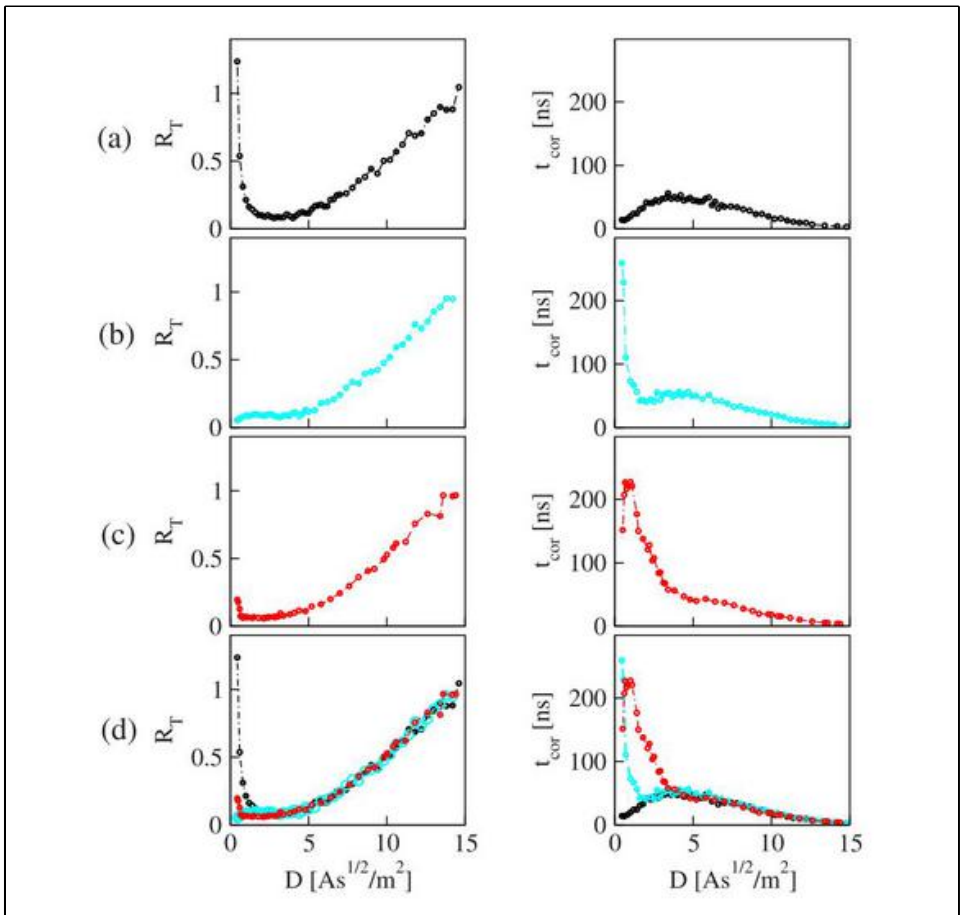

K = 0

nichtopt. τ → Kohärenzresonanz zerstört

optimales τ → Kohärenzresonanz verstärkt

(beide im delay-induz. Oszillationsregime)

FIG. 7. (Color online) Correlation time (right) and normalized fluctuation of pulse durations (left) as a function of the noise intensity for (a) $K=0$, (b) $(K,\tau)=(0.02\ \mathrm{V\,mm^2/A}, 11\ \mathrm{ns})$, and (c) $(K,\tau)=(0.02\ \mathrm{V\,mm^2/A}, 14.5\ \mathrm{ns})$. All three curves are plotted together in (d). Averages over 30 time series realizations of length $T=1600$ ns have been used for the calculation of t_{cor} and averages over 1000 periods for R_T. $U=2.99$ V and $\sigma=2.0821\ (\Omega\,\mathrm{m})^{-1}$.

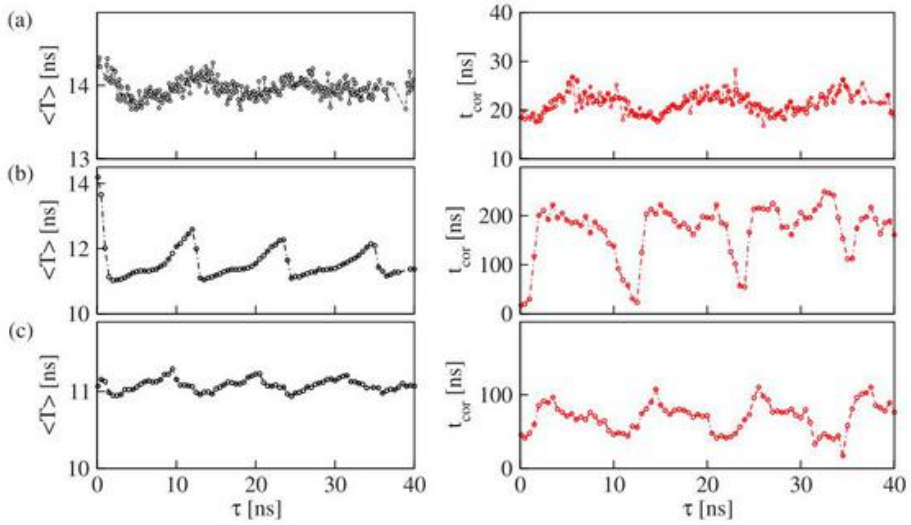

FIG. 6. (Color online) Mean interspike interval $\langle T\rangle$ (left) and correlation time t_{cor} (right) in dependence on the time delay τ. (a) Control strength $K=0.002\ \mathrm{V\,mm^2/A}$ and noise intensity $D=1.0\ \mathrm{A\,s^{1/2}/m^2}$, (b) $K=0.02\ \mathrm{V\,mm^2/A}$ and $D=1.0\ \mathrm{A\,s^{1/2}/m^2}$, and (c) $K=0.02\ \mathrm{V\,mm^2/A}$ and $D=2.5\ \mathrm{A\,s^{1/2}/m^2}$. Averages over 30 time series realizations of length $T=1600$ ns have been used for the calculation of t_{cor} and averages over 1000 periods for $\langle T\rangle$. $U=2.99$ V and $\sigma=2.0821\ (\Omega\,\mathrm{m})^{-1}$.

zu kleines K

kleine Rauschint.

große Rauschint.

2. Resonante Tunneldiode

Stegemann, Balanov, Schöll: PRE 71, 016220 (2005)
PRE 73, 016203 (2006)
Majer, Schöll: PRE 79, 011109 (2009)

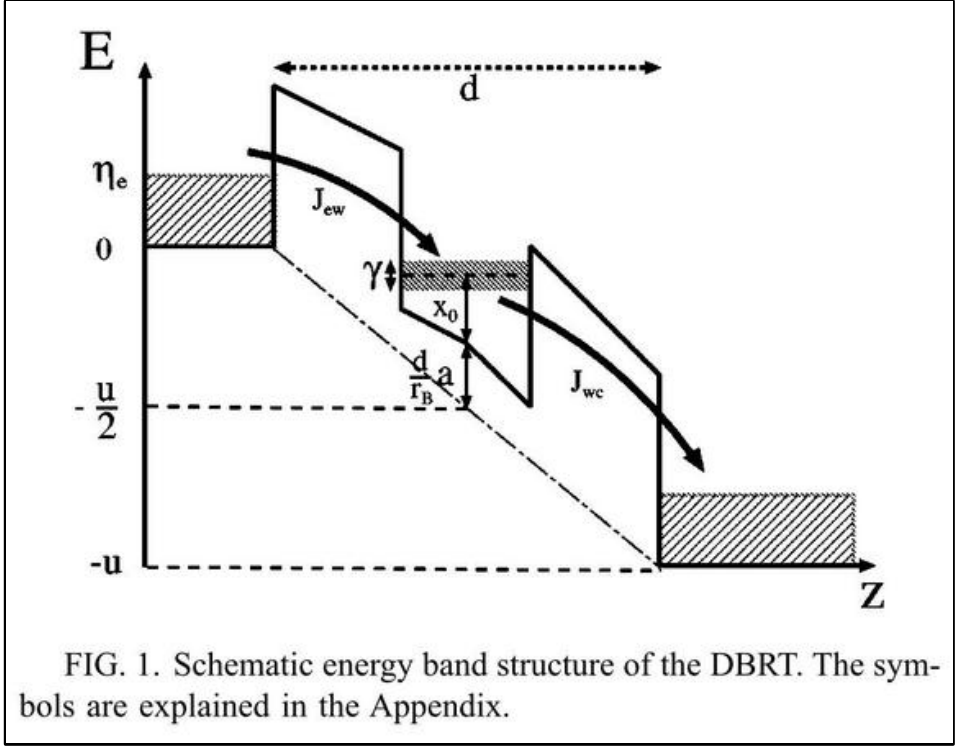

FIG. 1. Schematic energy band structure of the DBRT. The symbols are explained in the Appendix.

Double Barrier Resonant Tunnel Diode (DBRT)

Bandverbiegung durch Ladungsaustausch im QW

⇒ Z-förmige N-förmige I-U-Char.

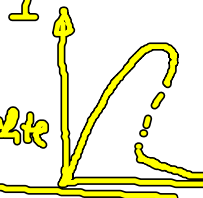

$$\dot{a} = f(a,u) + D\frac{d^2}{dx^2}a + D_a\,\xi(x,t)$$ Ladungsdichte

$$\dot{u} = \frac{1}{\varepsilon}\left(U_0 - u - RJ\right) + D_u\,\eta(t) + K[u(t-\tau) - u(t)]$$ Kirchhoff-Gl.

$\varepsilon = \frac{RC}{\tau_a}$

Rückkopplung über Schaltung

Reaktions-Diff.-Modell mit globaler Kopplung

- raum-zeitl. Osz. (breathing current filaments) durch Hopf-Bif. ($D = K = 0$)
- knapp unterhalb der Hopf-Bif.: rauschinduz. breathing ($K = 0$)

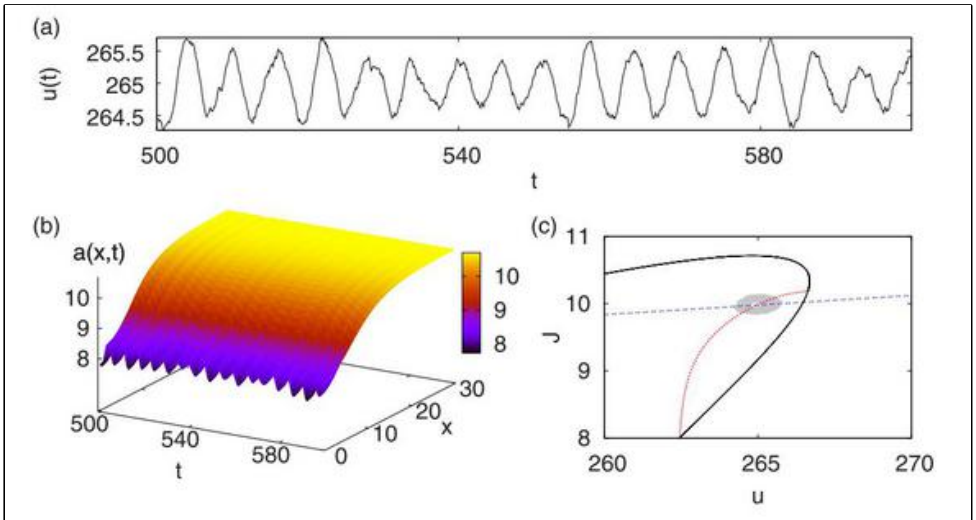

FIG. 1. (Color online) Stochastic spatiotemporal dynamics under multiple time-delayed feedback control. (a) Voltage time series $u(t)$ (in units of 0.35 mV), (b) charge carrier density $a(x,t)$ (in units of $10^{10}/\mathrm{cm}^2$), (c) phase portrait of current J (in units of 500 $\mathrm{A/cm}^2$) vs voltage u. Space x and time t are scaled in units of 100 nm and

vs voltage u. Space x and time t are scaled in units of 100 nm and 3.3 ps, respectively, corresponding to typical device parameters at 4 K [29]. Parameters are $U_0=-84.2895$, $r=-35$, $\varepsilon=6.2$, $D_u=0.1$, $D_a=10^{-4}$, $K=0.1$, $\tau=6.3$, $R=0.5$.

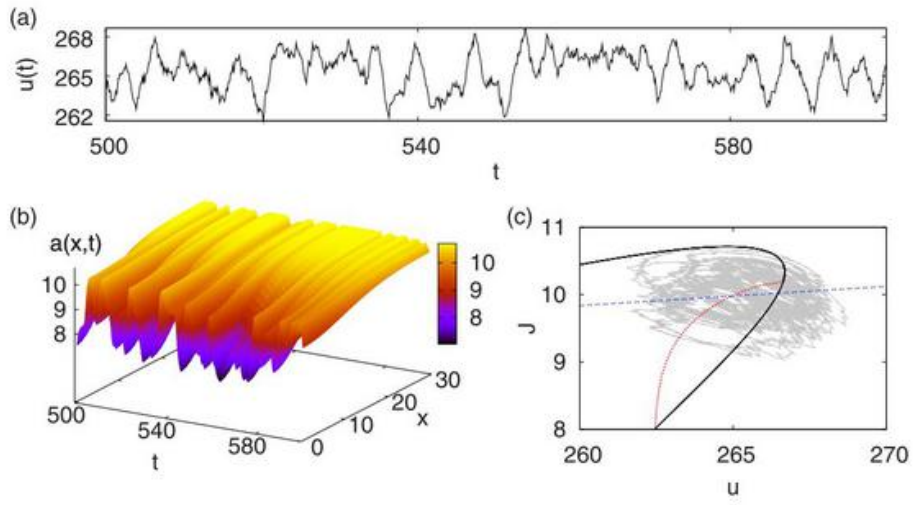

FIG. 2. (Color online) Same as Fig. 1 for $D_u=1.0$.

- Vergrößerung von t_{cor} w.r.t τ durch opt. τ

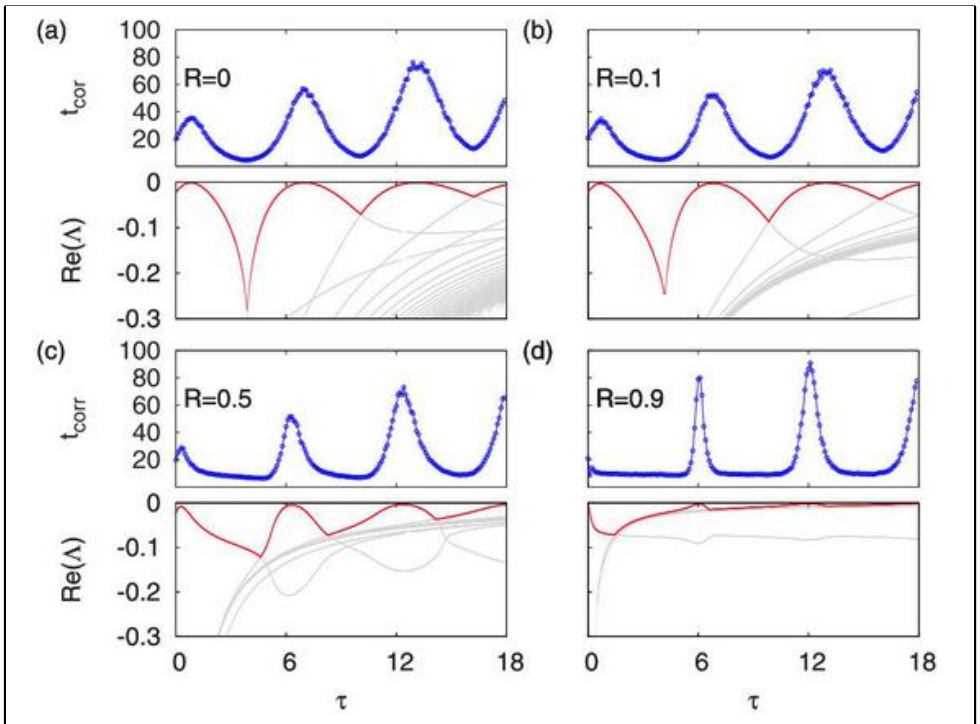

FIG. 7. (Color online) Correlation times t_{cor} (upper panels) and deterministic stability of the inhomogeneous fixed point, Re(Λ) (lower panels), in dependence of the delay time τ for different values of the memory parameter R [(a)–(d)] and fixed $K=0.1$. The red (dark) curves in the lower panels mark the leading eigenvalue, which governs the overall stability of the fixed point. Parameters: $\varepsilon=6.2$, $D_u=0.1$, and $D_a=10^{-4}$ (in the panels showing t_{cor}).

6. Kontrolle in optischen Systemen

6.1 Laser & Kontrolle

6.2 Rauschunterdrückung im Laser

6.3 zeitverzögert gekoppelte Laser

6.1 Laser & Kontrolle

Beschreibung: semiklassische Gleichungen

- Elektrisches Feld: klassisch (Maxwell-Gleichungen)
- Atome: quantentheoretisch (Besetzungsinversion und ggf. Polarisation der Atome aus Schrödinger-Gleichung)

hier: adiabatische Eliminierung der Polarisation

$\left(\frac{1}{\tau_{Pol.}} \gg \frac{1}{\tau_{Feld}}\right.$: Polarisation folgt instantan$\Big)$

Lang-Kobayashi-Gleichungen:

Ref.: R. Lang, K. Kobayashi, IEEE J. Quantum Electronics 16, 347 (1980)

$$\frac{dE}{dt} = \frac{1}{2}(1+i\alpha)\,n\,E - E_b + F_E$$

$$T\frac{dn}{dt} = I - n - (1+n)\,k(n)\,|E|^2$$

Variablen & Parameter:

E : Komplexes elektrisches Feld (slowly varying envelope approximation amplitude)

und $|E|^2$ Intensität

α : linewidth enhancement factor

n : Ladungsträgerdichte (Inversion relativ zur Laser-Schwelle bei $n_{th} \stackrel{!}{=} 0$)

T : Zeitskalenparameter $\frac{\tau_{carrier}}{\tau_{photon}} \approx 10^3$

I : Pumpstrom

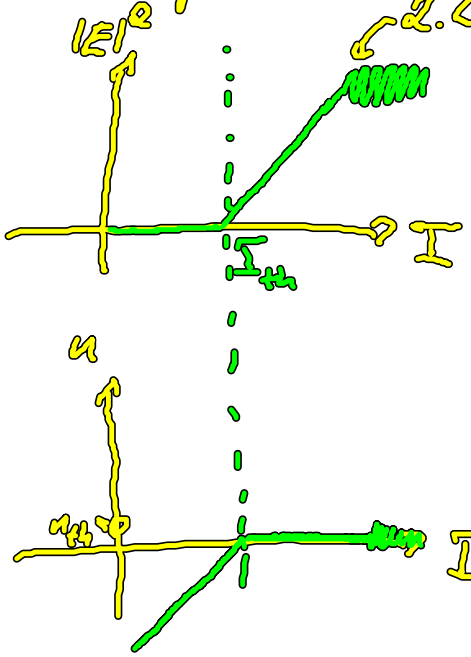

⇒ Intensitätsoszillationen oberhalb einer Hopf-Bifurkation

in Gleichungen berücksichtigt durch

$k(n)$ (passives, internes feedback im Laser mit „bragg grating")

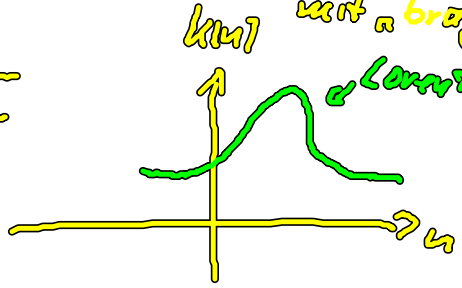

$$k(n) = k_0 + \frac{A w^2}{4(n-n_0)^2 + w^2}$$

zusätzliche Einflüsse:

E_b : optisches feedback analog zu Pyragas-Kontrolle

$$E_b(t) = \kappa e^{i\varphi} \sum_{m=0}^{\infty} R^m \left[E(t - \delta - m\tau) - E(t - \delta - (m+1)\tau) \right]$$

F_E : Rauschterm (⇒ 6.2)

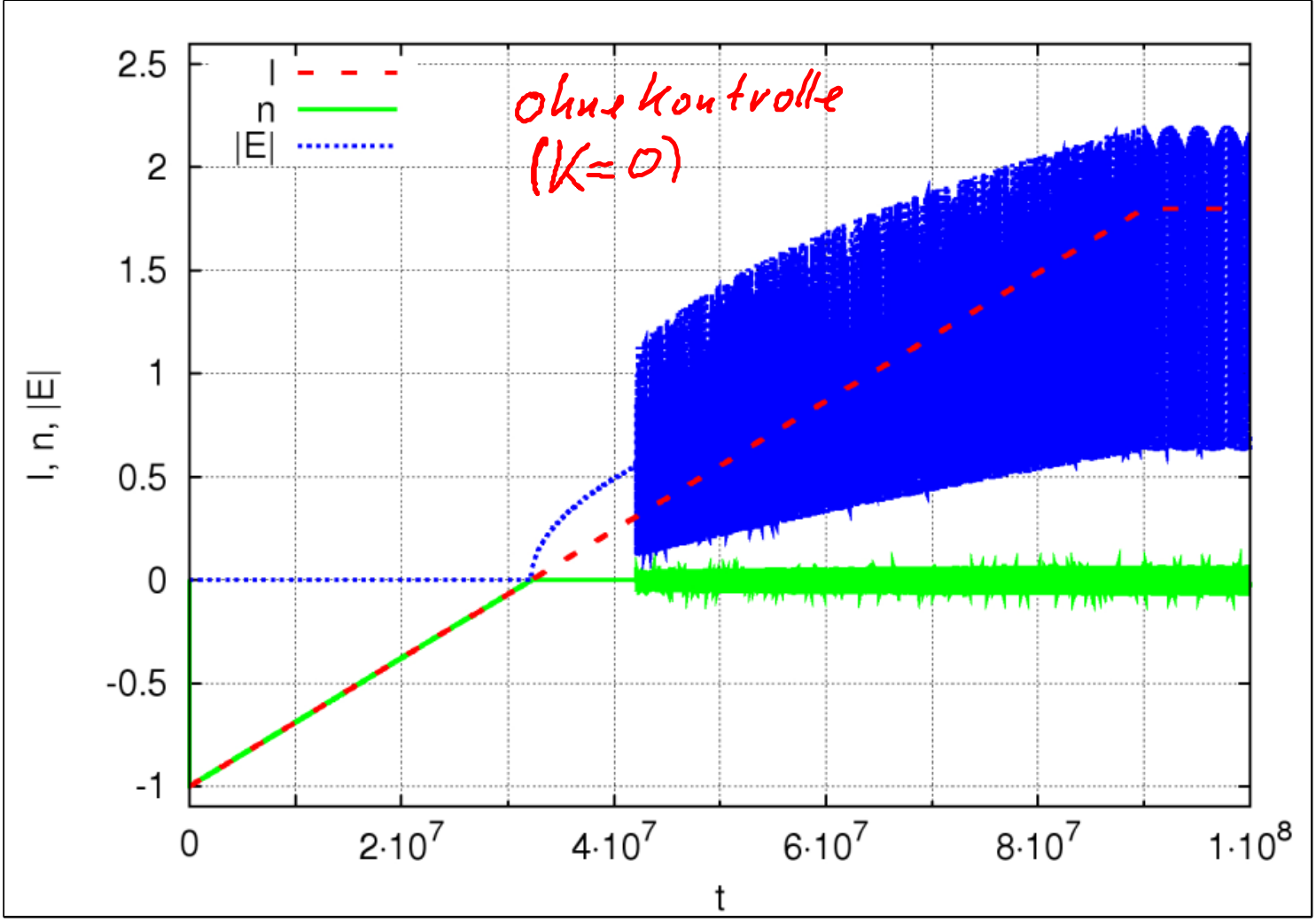
I
n
|E|
ohne Kontrolle
(K=0)
I, n, |E|
t
2.5
2
1.5
1
0.5
0
-0.5
-1
0
2·10^7
4·10^7
6·10^7
8·10^7
1·10^8

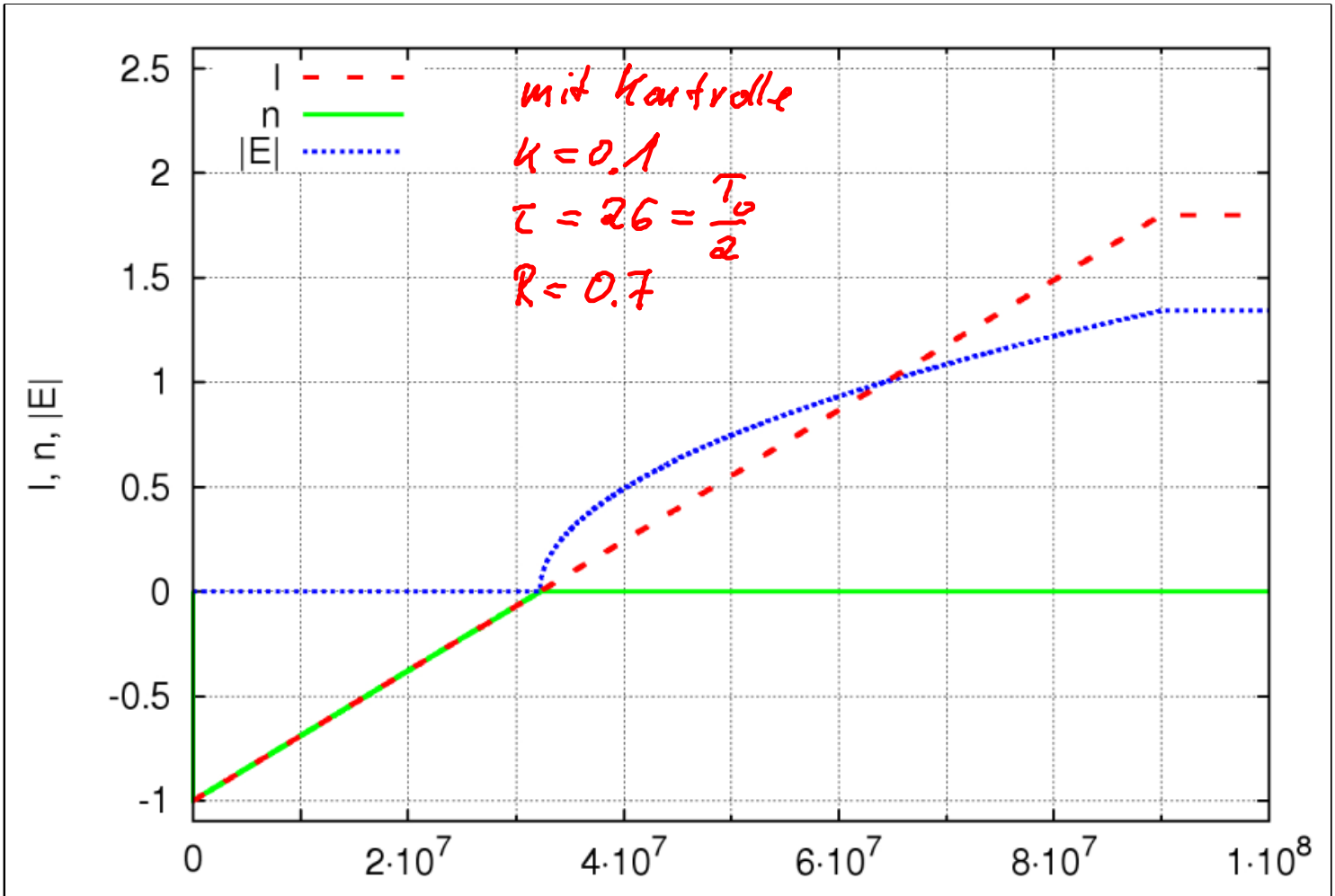
I
n
|E|
mit Kontrolle
K = 0.1
τ = 26 = T0/2
R = 0.7
I, n, |E|
2.5
2
1.5
1
0.5
0
-0.5
-1
0
2·10^7
4·10^7
6·10^7
8·10^7
1·10^8

t